Mathematics

http://www.aimspress.com/journal/Math

AIMS Mathematics, 7(4): 5156–5174.
DOI:10.3934/math.2022288
Received: 10 September 2021
Revised: 02 November 2021
Accepted: 21 November 2021
Published: 04 January 2022

Research article

Fractional order COVID-19 model with transmission rout infected through environment

Shao-Wen Yao[1], **Muhammad Farman**[2], **Maryam Amin**[2], **Mustafa Inc**[3,4,5,*], **Ali Akgül**[6] **and Aqeel Ahmad**[2]

[1] School of Mathematics and Information Science, Henan Polytechnic University, Jiaozuo 454000, China
[2] Department of Mathematics and Statistics, University of Lahore, Lahore-54590, Pakistan
[3] Department of Computer Engineering, Biruni University, 34025 Istanbul, Turkey
[4] Department of Mathematics, Science Faculty, Firat University, 23119 Elazig, Turkey
[5] Department of Medical Research, China Medical University, 40402 Taichung, Taiwan
[6] Art and Science Faculty, Department of Mathematics, Siirt University, 56100 Siirt, Turkey

* **Correspondence:** Email: minc@firat.edu.tr.

Abstract: In this paper, we study a fractional order COVID-19 model using different techniques and analysis. The sumudu transform is applied with the environment as a route of infection in society to the proposed fractional-order model. It plays a significant part in issues of medical and engineering as well as its analysis in community. Initially, we present the model formation and its sensitivity analysis. Further, the uniqueness and stability analysis has been made for COVID-19 also used the iterative scheme with fixed point theorem. After using the Adams-Moulton rule to support our results, we examine some results using the fractal fractional operator. Demonstrate the numerical simulations to prove the efficiency of the given techniques. We illustrate the visual depiction of sensitive parameters that reveal the decrease and triumph over the virus within the network. We can reduce the virus by the appropriate recognition of the individuals in community of Saudi Arabia.

Keywords: COVID-19 model; transmission rout; uniqueness; stability; sumudu transform; Adams-Moulton rule; fractal fractional
Mathematics Subject Classification: 37C75, 65L07, 93B05

1. Introduction

Mathematical models are known to address and answer specific questions for the disease under consideration. For example, for the prediction of the spread of infectious diseases, epidemiological models are very supportive. To control the disease, it assists the community to notice sensitive features. We aim to explore one of these models to study the behavior of the virus COVID-19 that appeared in early 2020 and is still not fully controlled. For the better understanding of physical phenomena, we look into fractional calculus. Several operators were demonstrated in the literature [1, 2] with the help of fractional calculus. Few implementations of these operators can be seen in [3–7]. In C^{η}-Calculus, Golmankhaneh et al. [8] explained the Sumudu transform and Laplace. In 2019, with the help of the fractional model, Goyal provided an approach [9] to control the Lassa hemorrhagic fever disease. In China, Zhao et al. [10] formulated a model to control COVID-19. It spreads from person to person via connection with the contaminated person using breathing the same air, coughing, sneezing, touching, and touching the same surfaces. The prime prevention approaches are wearing a mask in public at all times, washing your hands, and maintaining a proper distance from anyone. A well-defined approach of the fractional-order model is described in [11]. Some fractional models of COVID-19 are coming up recently, in which Atangana and Khan [12] have investigated the condition of China due to pandemics. In [13], by considering Fuzzy Caputo and ABC derivative founders look into the dynamical study of the COVID-19 model. Further, the writers measured the model of COVID in the Caputo operator [14]. Using actual data from March 02 to April 14 [15], Alshammari also contributed to the pandemic. To enforce the fractional model [16–18], the investigator applied the homotopy analysis transform method (HATM), and the comparison showed that this technique is highly effective. In [17], stability of fractal differentials in the sense of Lyapunov is defined. Moreover, based on the fractal set, they generalized the non-local fractional integrals and derivatives. A hybrid method based on operational matrices of the derivative is proposed and successfully applied to explore the solution of the mobile–immobile advection-dispersion problem of variable order [19]. similarly, Work with exact solutions and existing methods included numerical and analytical was made [20] that showed an excellent level of accuracy for the problems. Some applications of fractional order model with local and non-local nonsingular kernel have also been studied in [21–27]. Padmavathi et al. [28] also worked on the q-HATM with the latest operator Atangana-Baleanue to get finer recognization, and they expressed their results in the form of visualization. For the set up of operational matrices, a piecewise function was deployed in [29]. Also, for implementation in a simple way, researchers converted the design into a linear system. In [30], a fractional Biswas-Milovic model was inspected through the technique of fractional complex transform. To analyze the nonlinear oscillatory fractional-order differential equation, A spectral approach through the Chelyshkov polynomial method (CPM) and Picard iterative (PI) was used [31]. Mehmood et al. [32] used the techniques Galerkin-Petrove (G-P) and Rung Kutta (RK) to study the model and they concluded that in comparison, the G-P technique is better. The effect of vaccination of COVID-19 through different values of parameters had studied in [33]. The common SEIR model is generalized in order to show the dynamics of COVID-19 transmission taking into account the ABO blood group of the infected people. Fractional order Caputo derivative are used in the proposed model [34].

Some basic definitions of fractional calculus are described in Section 2. Later, a fractional-order COVID-19 model is presented in Section 3. Moreover, sensitivity analysis of the model and some theorems are added. Further in Section 4, the simulations are demonstrated. The last section consists of a conclusion.

2. Materials and methods

In this section, some primary notions have been described that are helpful to analyze the system.
Definition 1. For $z \in H^1(x,y)$ and $\kappa \in (0,1)$. The Caputo-Fabrizio fractional derivative [35] is defined as

$$ {}^{CF}D_t^{\kappa}\Big(z(t)\Big) = \frac{M(\kappa)}{1-\kappa}\int_x^t z^{'}(\rho)exp\Big[-\kappa\frac{t-\rho}{1-\kappa}\Big] \tag{2.1}$$

where $M(\kappa)$ is a normalization function.
Definition 2. Antagana-Baleanu in Caputo sense (ABC) can be defined [36] as

$$ {}_{\alpha}^{ABC}D_t^{\alpha}(\psi(t)) = \frac{AB(\alpha)}{n-\alpha}\int_{\alpha}^{\chi}\frac{d^n}{dw^n}f(w)E_{\alpha}\left(-\alpha\frac{(\chi-w)^{\alpha}}{n-\alpha}\right)dw,\ n-1<\alpha<n, \tag{2.2}$$

where E_{α} is the Mittag-Leffler function and $AB(\alpha)$ is a normalization function. For Eq (2.2), a Laplace transformation is presented as:

$$ L[{}_{\alpha}^{ABC}D_t^{\alpha}(\psi(t))](S) = \frac{AB(\alpha)}{1-\alpha}\frac{S^{\alpha}L[\psi(\tau)](S)-S^{\alpha-1}\psi(0)}{S^{\alpha}+\frac{\alpha}{1-\alpha}}. \tag{2.3}$$

For using ST for (2.2), we obtain

$$ ST[{}_0^{ABC}D_t^{\alpha}(\psi(t))](S) = \frac{B(\alpha)}{1-\alpha+\alpha S^{\alpha}}[ST\psi(t)-\psi(0)]. \tag{2.4}$$

Definition 3. Atangana-Baleanu fractional integral of order μ of a function $\psi(t)$ can be expressed as [37]

$$ {}_{\mu}^{ABC}I_{\chi}^{\mu}(\psi(\chi)) = \frac{1-\mu}{B-\mu}\psi(\chi) + \frac{\mu}{B(\mu)\Gamma(\mu)}\int_{\alpha}^{\chi}\psi(S)(\chi-S)^{\mu-1}ds. \tag{2.5}$$

3. Fractional order COVID-19 model

The current section investigates the displaying of the novel Coronavirus. We start the demonstrating interaction be meaning the host populace by $N(t)$ dividing into five totally unrelated epidemiological classes based on dynamics of COVID-19 contamination. These classes comprise of susceptible S, exposed U, irresistible appearance indications of disease C, contaminated with no illness symptoms C_a and the people recuperated are denoted R respectively. Classical order Covid-19 model is given in [38] and fractional order form with ABC sense is shown in followings equation

$$\begin{aligned}
{}_0^{ABC}D_t^{\alpha}S(t) &= H-\Big(\mu_1U+\mu_2C+\mu_3C_a+\mu_4B\Big)\frac{S}{N}-bS,\\
{}_0^{ABC}D_t^{\alpha}U(t) &= \Big(\mu_1U+\mu_2C+\mu_3C_a+\mu_4B\Big)\frac{S}{N}-\Big(\rho+b\Big)U,\\
{}_0^{ABC}D_t^{\alpha}C(t) &= \rho\Big(1-\tau\Big)U-\Big(b+c_1+d_1\Big)C,\\
{}_0^{ABC}D_t^{\alpha}C_a(t) &= \tau\rho U-\Big(b+d_2\Big)C_a, \qquad (3.1)
\end{aligned}$$

$$\begin{aligned} {}_0^{ABC}D_t^{\alpha}R(t) &= d_1C + d_2C_a - bR, \\ {}_0^{ABC}D_t^{\alpha}B(t) &= \phi_1U + \phi_2C + \phi_3C_a - \sigma B. \end{aligned}$$

With initial condintion

$$S(0) \geq 0,\ U(0) \geq 0,\ C(0) \geq 0,\ C_a(0) \geq 0,\ R(0) \geq 0,\ B(0) \geq 0.$$

Here H, b, and μ are represents birth rate, passing rate in each class and infected rate respectively. The parameters μ_1, μ_2 and μ_3 are the viable transmission paces of contamination due to exposed, symptomatically-infected and symptomatically-infected individuals, respectively. μ_4 denotes the age of infection due to climate. We denote the incubation period of the individuals by ρ. d_1 and d_2 are represents the recovery rates from infected population. The contribution of the virus to the environment due to exposed, and the population of both infected compares (i.e., C and C_a) are shown respectively by ϕ_1, ϕ_2 and ϕ_3. We have

$$\lambda(t) = \frac{(\mu_1U + \mu_2C + \mu_3C_a + \mu_4B)}{N},\quad l_1 = (\rho + b),$$
$$l_2 = (b + c_1 + d_1),\quad l_3 = (b + d_2).$$

From above, we have

$$\begin{aligned} {}_0^{ABC}D_t^{\alpha}S(t) &= \Pi - \lambda(t)S - bS, \\ {}_0^{ABC}D_t^{\alpha}U(t) &= \lambda(t)S - l_1U, \\ {}_0^{ABC}D_t^{\alpha}C(t) &= \rho(1-\tau)U - k_2C, \\ {}_0^{ABC}D_t^{\alpha}C_a(t) &= \tau\rho U - k_3C_a, \\ {}_0^{ABC}D_t^{\alpha}R(t) &= d_1C + d_2C_a - bR, \\ {}_0^{ABC}D_t^{\alpha}B(t) &= \phi_1U + \phi_2C + \phi_3C_a - \sigma B. \end{aligned} \tag{3.2}$$

3.1. Equilibria and sensitivity analysis

We define corona free equilibria as:

$$M_1 = \left(S^1, U^1, C^1, C_a^1, R^1, B^1\right) = \left(\frac{H}{b}, 0, 0, 0, 0, 0\right) \tag{3.3}$$

and the corona existing equilibria as:

$$M_2 = \left(S^*, U^*, C^*, C_a^*, R^*, B^*\right) \tag{3.4}$$

we get S^*, U^*, C^*, C_a^*, R^*, B^* as:

$$S^* = \frac{H}{\lambda + b},\quad U^* = \frac{\lambda S^*}{\rho + b},\quad C^* = \frac{(1-\tau)\rho U^*}{b + c_1 + d_1},\quad C_a^* = \frac{\tau\rho U^*}{b + d_2},$$

$$R^* = \frac{d_1C^* + d_2C_a^*}{b},\quad B^* = \frac{\phi_1U^* + +\phi_2C* + \phi_3C_a*}{\sigma B} \tag{3.5}$$

where

$$\lambda^* = \frac{(\mu_1 U^* + \mu_2 C^* + \mu_3 C_a^* + \mu_4 B^*)}{N^*} \tag{3.6}$$

By substituting (3.5) into (3.6), we get λ^* as:

$$Z_1\lambda^* + Z_2 = 0, \tag{3.7}$$

where

$$Z_1 = \sigma\Big(\rho l_3(b + d_1)(1 - \tau) + l_2(\rho\tau(d_2 + b) + bl_3)\Big),$$

$$Z_2 = l_1 l_2 l_3 b\sigma(1 - R_0). \tag{3.8}$$

For the derivation, the reproduction number R_0 is the spectral radius of $Y * Z^{-1}$, where Y and Z are the transmission and the transition matrices respectively. Thus, we get

$$R_0 = \frac{\rho(1-\tau)(\mu_4\phi_2 + \mu_2\sigma)}{l_1 l_2 \sigma} + \frac{\rho\tau(\mu_4\phi_3 + \mu_3\sigma)(\mu_4\phi_2 + \mu_2\sigma)}{l_1 l_3 \sigma} + \frac{\mu_4\phi_1 + \mu_1\sigma}{l_1\sigma} \tag{3.9}$$

or

$$R_0 = \frac{l_2[\rho\tau(\mu_4\phi_2 + \mu_3\sigma) + l_3(\mu_4\phi_1 + \mu_1\sigma)] + \rho l_3(1-\tau)(\mu_4\phi_2 + \mu_2\sigma)}{l_1 l_2 l_3 \sigma} \tag{3.10}$$

Sensitivity of R_0 can be analyzed by taking the partial derivatives of reproductive number for the involved parameters as follows

$$\begin{aligned}
\frac{\partial R_0}{\partial \rho} &= \frac{(l_1 l_2 l_3 \sigma[l_2\tau(\mu_4\phi_2 + \mu_3\sigma) + l_3(1-\tau)(\mu_4\phi_2 + \mu_2\sigma)]}{(l_1 l_2 l_3 \sigma)^2} > 0,\\
\frac{\partial R_0}{\partial \tau} &= \frac{(l_1 l_2 l_3 \rho\sigma[l_2(\mu_4\phi_2 + \mu_3\sigma) - l_3(\mu_4\phi_2 + \mu_2\sigma)]}{(l_1 l_2 l_3 \sigma)^2} > 0,\\
\frac{\partial R_0}{\partial l_1} &= -\frac{l_2 l_{3\sigma}[(l_2(\rho\tau(\mu_4\phi_2 + \mu_3\sigma) + l_3(\mu_4\phi_1 + \mu_1\sigma)) + \rho l_3(1-\tau)(\mu_4\phi_2 + \mu_2\sigma)]}{(l_1 l_2 l_3 \sigma)^2} < 0,\\
\frac{\partial R_0}{\partial l_2} &= -\frac{[(l_1 l_2 l_3^2 \sigma(\mu_4\phi_1 + \mu_1\sigma) + (l_1 l_3^2 \rho\sigma(1-\tau)(\mu_4\phi_2 + \mu_2\sigma)]}{(l_1 l_2 l_3 \sigma)^2} < 0,\\
\frac{\partial R_0}{\partial l_3} &= \frac{l_1 l_3 \sigma(\mu_4\phi_1 + \mu_1\sigma)[l_3 - l_2\rho\tau]}{(l_1 l_2 l_3 \sigma)^2} > 0,
\end{aligned}$$

$$\begin{aligned}
\frac{\partial R_0}{\partial \mu_1} &= \frac{1}{l_1 l_2} > 0,\\
\frac{\partial R_0}{\partial \mu_2} &= \frac{\rho(1-\tau)}{l_1 l_2} > 0,\\
\frac{\partial R_0}{\partial \mu_3} &= \frac{1}{l_1 l_3} > 0,\\
\frac{\partial R_0}{\partial \mu_4} &= \frac{l_2\rho\tau\phi_2 + l_3\phi_1 + \rho l_3(1-\tau)\phi_2}{l_1 l_2 l_3 \sigma} > 0,
\end{aligned}$$

$$\frac{\partial R_0}{\partial \phi_1} = \frac{\mu_4}{l_1 l_2 \sigma} > 0,$$
$$\frac{\partial R_0}{\partial \phi_2} = \frac{\rho\mu_4[l_2\tau - l_3(1-\tau)]}{l_1 l_2 l_3 \sigma} > 0,$$
$$\frac{\partial R_0}{\partial \sigma} = -\frac{l_1 l_2 l_3 \mu_4[l_2\rho\tau\phi_2 + l_3\phi_1 + \rho l_3(1-\tau)\phi_2]}{(l_1 l_2 l_3 \sigma)^2} < 0.$$

Clearly, in case of change in parameter R_0 is very sensitive. In this manuscript, $\rho,\ \tau,\ l_3,\ \mu_1,\ \mu_2,\ \mu_3,\ \mu_4,$ $\phi_1,\ \phi_2$ are growing while $l_1,\ l_2,\ \sigma$ are reducing. Thus, based on sensitivity analysis, we can say that prevention is better to control the disease.

Theorem 1. For a Banach Space $(G, |.|)$ and F is a self-map of K fulfilling

$$||F_X - F_r|| \leqslant \theta||G - F_G|| + \theta||G - r||. \tag{3.11}$$

$\forall\ G,\ r \in G$ where $0 \le \theta \le 1$. Let F be a Picard F-stable.

We take into consideration Eq (3.2) and get

$$\frac{1-\alpha}{B(\alpha)\alpha\Gamma(\alpha+1)E_\alpha\left(-\frac{1}{1-\alpha}W^\alpha\right)} = \frac{1-\alpha}{Y} \tag{3.12}$$

Theorem 2. We describe F as a self-map by

$$\begin{aligned}
F[S_{(w+1)}(t)] &= S_{(w+1)}(t) = S_w(0) + ST^{-1}\Big[\frac{1-\alpha}{Y} \times ST\Big\{H - \frac{(\mu_1 E + \mu_2 I + \mu_3 I_a + \mu_4 B)}{N}S - bS\Big\}\Big],\\
F[U_{(w+1)}(t)] &= U_{(w+1)}(t) = U_w(0) + ST^{-1}\Big[\frac{1-\alpha}{Y} \times ST\Big\{\frac{(\mu_1 U + \mu_2 C + \mu_3 C_a + \mu_4 B)}{N}S - (\rho + b)U\Big\}\Big],\\
F[C_{(w+1)}(t)] &= C_{(w+1)}(t) = C_w(0) + ST^{-1}\Big[\frac{1-\alpha}{Y} \times ST\Big\{\rho(1-\tau)U - (b + c_1 + d_1)C\Big\}\Big],\\
F[C_{a(w+1)}(t)] &= C_{a(w+1)}(t) = C_{a(w)}(0) + ST^{-1}\Big[\frac{1-\alpha}{Y} \times ST\Big\{\tau\rho U - (b + \delta_2)C_a\Big\}\Big],\\
F[R_{(w+1)}(t)] &= R_{(w+1)}(t) = R_w(0) + ST^{-1}\left[\frac{1-\alpha}{Y} \times ST\Big\{d_1 I + d_2 C_a - bR\Big\}\right]\\
F[B_{(w+1)}(t)] &= B_{(w+1)}(t) = B_w(0) + ST^{-1}\left[\frac{1-\alpha}{Y} \times ST\Big\{\phi_1 U + \phi_2 C + \phi_3 C_a - \sigma B\Big\}\right],
\end{aligned} \tag{3.13}$$

Then, we reach

$$||F[S_w(t)] - F[S_x(t)]|| \le ||S_w(t) - S_x(t)|| + ST^{-1}\Bigg[\frac{1-\alpha}{Y}\times$$
$$ST\Big\{H - \frac{(\mu_1||U_w(t) - U_x(t)|| + \mu_2||C_w(t) - C_x(t)|| + \mu_3||C_w(t) - C_x(t)|| + mu_4||B_w(t) - B_x(t)||)}{N}$$
$$||S_w(t) - S_x(t)|| - b||S_w(t) - S_x(t)||\Big\}\Bigg],$$

$$\|F[U_w(t)] - F[U_x(t)]\| \le \|U_w(t) - U_x(t)\| + ST^{-1}\Bigg[\frac{1-\alpha}{Y}\times$$
$$ST\Big\{\frac{(\mu_1\|U_w(t) - U_x(t)\| + \mu_2\|C_w(t) - C_x(t)\| + mu_3\|C_w(t) - C_x(t)\| + mu_4\|B_w(t) - B_x(t)\|)}{N}$$
$$\|S_w(t) - S_x(t)\| - (\rho + b)\|U_w(t) - U_x(t)\|\Big\}\Bigg],$$

$$\|F[C_w(t)] - F[C_x(t)]\| \le \|C_w(t) - C_x(t)\| + ST^{-1}\Bigg[\frac{1-\alpha}{Y}$$
$$\times ST\Big\{\rho(1-\tau)\|U_w(t) - U_x(t)\| - (b + c_1 + d_1)\|C_w(t) - C_x(t)\|\Big\}\Bigg],$$

$$\|F[C_{a(w)}(t)] - F[C_{a(x)}(t)]\| \le \|C_{a(w)}(t) - C_{a(x)}(t)\| + ST^{-1}$$
$$\Bigg[\frac{1-\alpha}{Y}\times ST\Big\{\tau\rho\|U_w(t) - U_x(t)\| - (b + d_2)\|C_{a(w)}(t) - C_{a(x)}(t)\|\Big\}\Bigg],$$

$$\|F[R_w(t)] - F[R_x(t)]\| \le \|R_w(t) - R_x(t)\| + ST^{-1}\Bigg[\frac{1-\alpha}{Y}$$
$$\times ST\Big\{d_1\|C_w(t) - C_x(t)\| + d_2\|C_{a(w)}(t) - C_{a(x)}(t)\| - b\|R_w(t) - R_x(t)\|\Big\}\Bigg],$$

$$\|F[B_w(t)] - F[B_x(t)]\| \le \|B_w(t) - B_x(t)\| + ST^{-1}\Bigg[\frac{1-\alpha}{Y}\times ST\Big\{\phi_1\|U_w(t) - U_x(t)\|$$
$$+\phi_2\|C_w(t) - C_x(t)\| + \phi_3\|C_{a(w)}(t) - C_{a(x)}(t)\| - \sigma\|B_w(t) - B_x(t)\|\Big\}\Bigg].$$

F satisfies the condition associated with Theorem 1 if

$$\theta(0,0,0,0,0,0),\theta=\begin{cases}\|S_w(t)-S_x(t)\|\times\|-(S_w(t)-S_x(t))\|+H\\ -\frac{(\mu_1\|U_w(t)-U_x(t)\|+\mu_2\|C_w(t)-C_x(t)\|+\mu_3\|C_w(t)-C_x(t)\|+\mu_4\|B_w(t)-B_x(t)\|)}{N}\|S_w(t)-S_x(t)\|\\ -b\|S_w(t)-S_x(t)\|,\\ \|U_w(t)-U_x(t)\|\times\|-(U_w(t)-U_x(t))\|\\ +\frac{(\mu_1\|U_w(t)-U_x(t)\|+\mu_2\|C_w(t)-C_x(t)\|+\mu_3\|C_w(t)-C_x(t)\|+\mu_4\|B_w(t)-B_x(t)\|)}{N}\|S_w(t)-S_x(t)\|\\ -(\rho+\mu)\|E_w(t)-E_x(t)\|,\\ \|C_w(t)-C_x(t)\|\times\|(-C_w(t)-C_x(t))\|+\rho(1-\tau)\|U_w(t)-U_x(t)\|\\ -(b+c_1+d_1)\|C_w(t)-C_x(t)\|,\\ \|C_{a(w)}(t)-C_{a(x)}(t)\|\times\|-(C_{a(w)}w(t)-C_{a(x)}(t))\|+\tau\rho\|U_w(t)-U_x(t)\|\\ -(b+d_2)\|C_{a(w)}(t)-C_{a(x)}(t)\|,\\ \|R_w(t)-R_x(t)\|\times\|-(R_w(t)-R_x(t))\|+d_1\|C_w(t)-C_x(t)\|\\ +d_2\|C_{a(w)}(t)-C_{a(x)}(t)\|-b\|R_w(t)-R_x(t)\|,\\ \|B_w(t)-B_x(t)\|\times\|-(B_w(t)-B_x(t))\|+\phi_1\|U_w(t)-U_x(t)\|\\ +\phi_2\|C_w(t)-C_x(t)\|+\phi_3\|C_{a(w)}(t)-C_{a(x)}(t)\|-\sigma\|B_w(t)-B_x(t)\|.\end{cases}$$

We add that F is Picard k-stable.

Theorem 3. If we use the technique of recurrence then the system (3.2) posses a particular singular solution.

Proof. Assume Hilbert space $H=Z^2(x,w)\times(0,T))$ which can be defined as

$$h:((m,w)\times(0,T))\longrightarrow R,\int\int ghdgdh<\infty. \tag{3.14}$$

Then, we take into consideration:

$$\theta(0,0,0,0,0,0,),\theta=\begin{cases}H-\lambda(t)S-bS,\\ \lambda(t)S-l_1U,\\ \rho(1-\tau)U-l_2C,\\ \tau\rho U-l_3C_a,\\ d_1C+d_2C_a-bR,\\ \phi_1U++\phi_2C+\phi_3I_a-\sigma B.\end{cases} \tag{3.15}$$

We establish that the inner product of

$$T((S_{11}(t)-S_{12}(t),U_{21}(t)-U_{22}(t),C_{31}(t)-I_{32}(t),C_{a(41)}(t)-C_{a(42)}(t),R_{51}(t)-R_{52}(t),\\ B_{61}(t)-B_{62}(t),(V_1,V_2,V_3,V_4,V_5,V_6)),$$

where

$$\Big((S_{11}(t)-S_{12}(t)),(E_{21}(t)-E_{22}(t)),(I_{31}(t)-I_{32}(t)),(I_{a(41)}(t)-I_{a(42)}(t)),(R_{51}(t)-R_{52}(t)),$$

$$(B_{61}(t) - B_{62}(t))\Big)$$

are the special solution of the system. Then, we have

$$\begin{aligned}&\Big\{H - \lambda(t)(S_{11}(t) - S_{12}(t)) - b(S_{11}(t) - S_{12}(t)), V_1\Big\}\\ &\leq H\|V_1\| - \lambda(t)\|(S_{11}(t) - S_{12}(t))\|\|V_1\| + b\|(S_{11}(t) - S_{12}(t))\|\|V_1\|,\end{aligned}$$

$$\begin{aligned}&\Big\{\lambda(t)(S_{11}(t) - S_{12}(t)) - (\rho + b)(U_{21}(t) - U_{22}(t)), V_2\Big\}\\ &\leq \lambda(t)\|(S_{11}(t) - S_{12}(t))\|\|V_2\| + (\rho + b)\|U_{21}(t) - U_{22}(t)\|\|V_2\|,\end{aligned}$$

$$\begin{aligned}&\Big\{\rho(1 - \tau)(U_{21}(t) - U_{22}(t)) - (b + c_1 + d_1)(C_{31}(t) - C_{32}(t)), V_3\Big\}\\ &\leq \rho(1 - \tau)\|(U_{21}(t) - U_{22}(t)\|\|V_3\| + (b + c_1 + d_1)\|(C_{31}(t) - C_{32}(t)\|\|V_3\|,\end{aligned}$$

$$\begin{aligned}&\Big\{\tau\rho(U_{21}(t) - U_{22}(t)) - (b + d_2)(C_{a(41)}(t) - C_{a(42)}(t)), V_4\Big\}\\ &\leq \tau\rho\|(U_{21}(t) - U_{22}(t)\|\|V_4\| + (b + d_2)\|C_{a(41)}(t) - C_{a(42)}(t)\|\|V_4\|\end{aligned}$$

$$\Big\{d_1(C_{31}(t) - C_{32}(t)) + d_2(C_{a(41)}(t) - C_{a(42)}(t)) - b(R_{51}(t) - R_{52}(t)), V_5\Big\}$$

$$\leq d_1\|(C_{31}(t) - C_{32}(t)\|)\|V_5\| + d_2\|C_{a(41)}(t) - C_{a(42)}(t)\|\|V_5\| + b\|R_{51}(t) - R_{52}(t)\|\|V_5\|,$$

$$\Big\{\phi_1(U_{21}(t) - U_{22}(t)) + \phi_2(C_{31}(t) - C_{32}(t)) + \phi_3(C_{a(41)}(t) - C_{a(42)}(t)) - \sigma(B_{61}(t) - B_{62}(t)), V_6\Big\}$$

$$\leq \phi_1\|(U_{21}(t) - U_{22}(t)\|\|V_6\| + \phi_2\|(C_{31}(t) - C_{32}(t)\|)\|V_6\| + \phi_3\|C_{a(41)}(t) - C_{a(42)}(t)\|\|V_6\|$$

$$-\sigma\|(B_{61}(t) - B_{62}(t)\|\|V_6\|.$$

In case of large number e_1, e_2, e_3, e_4, e_5 and e_6, both solutions happen to be converged to the exact solution. By applying the concept of topology, we can get six positive very small variables (X_{e_1}, X_{e_2}, X_{e_3}, X_{e_4}, X_{e_5} and X_{e_6}.)

$$\begin{aligned}\|(S - S_{11}\|, \|S - S_{12}\| &\leq \frac{X_{e_1}}{\xi}, \|(U - U_{21}\|, \|U - U_{22}\| \leq \frac{X_{e_2}}{\zeta},\\ \|(C - C_{31}\|, \|C - C_{32}\| &\leq \frac{X_{e_3}}{\omega}, \|(C_a - C_{a(41)}\|, \|C_a - C_{a(42)}\| \leq \frac{X_{e_4}}{\varepsilon},\\ \|(R - R_{51}\|, \|R - R_{52}\| &\leq \frac{X_{e_5}}{\epsilon}, \|(B - B_{61}\|, \|B - B_{62}\| \leq \frac{X_{e_6}}{\varrho}\end{aligned}$$

where

$$\xi = 6\Big\{H - \lambda(t)\|(S_{11}(t) - S_{12}(t))\| + b\|(S_{11}(t) - S_{12}(t))\|\Big\}\|V_1\|,$$

$$\zeta = 6\Big\{\lambda(t)\|(S_{11}(t)-S_{12}(t))\| + (\rho+b)\|U_{21}(t)-U_{22}(t)\|\Big\}\|V_2\|,$$

$$\omega = 6\Big\{\rho(1-\tau)\|(U_{21}(t)-U_{22}(t)\| + (b+c_1+d_1)\|(C_{31}(t)-C_{32}(t)\|\Big\}\|V_3\|,$$

$$\varepsilon = 6\Big\{\tau\rho\|(U_{21}(t)-U_{22}(t)\| + (b+d_2)\|C_{a(41)}(t)-C_{a(42)}(t)\|)\Big\}\|V_4\|,$$

$$\epsilon = 6\Big\{d_1\|(C_{31}(t)-C_{32}(t)\|) + d_2\|C_{a(41)}(t)-C_{a(42)}(t)\| + b\|R_{51}(t)-R_{52}(t)\|)\Big\}\|V_5\|,$$

$$\varrho = 6\Big\{\phi_1\|(U_{21}(t)-U_{22}(t)\| + \phi_2\|(C_{31}(t)-C_{32}(t)\|) + \phi_3\|C_{a(41)}(t)-C_{a(42)}(t)\|$$

$$-\sigma\|(B_{61}(t)-B_{62}(t)\|)\Big\}\|V_6\|,$$

But it is obvious that

$$\Big(H - \lambda(t)\|(S_{11}(t)-S_{12}(t))\| + b\|(S_{11}(t)-S_{12}(t))\|\Big) \neq 0,$$

$$\Big(\lambda(t)\|(S_{11}(t)-S_{12}(t))\| + (\rho+b)\|U_{21}(t)-U_{22}(t)\|\Big) \neq 0,$$

$$\Big(\rho(1-\tau)\|(U_{21}(t)-U_{22}(t)\| + (b+c_1+d_1)\|(C_{31}(t)-C_{32}(t)\|)\Big) \neq 0,$$

$$\Big(\tau\rho\|(U_{21}(t)-U_{22}(t)\| + (b+d_2)\|C_{a(41)}(t)-C_{a(42)}(t))\Big) \neq 0,$$

$$\Big(d_1\|(C_{31}(t)-C_{32}(t)\|) + d_2\|C_{a(41)}(t)-C_{a(42)}(t)\| + b\|R_{51}(t)-R_{52}(t)\|\Big) \neq 0,$$

$$\Big(\phi_1\|(U_{21}(t)-U_{22}(t)\| + \phi_2\|(C_{31}(t)-C_{32}(t)\|) + \phi_3\|C_{a(41)}(t)-C_{a(42)}(t)\| - \sigma\|(B_{61}(t)-B_{62}(t)\|\Big) \neq 0,$$

where

$$\|V_1\|, \|V_2\|, \|V_3\|, \|V_4\|, \|V_5\|, \|V_6\| \neq 0.$$

Therefore, we have

$$\|S_{11}-S_{12}\| = 0, \|U_{21}-U_{22}\| = 0, \|C_{31}-C_{32}\| = 0,$$
$$\|C_{a(41)}-C_{a(42)}\| = 0, \|R_{51}-R_{52}\| = 0, \|B_{61}-B_{62}\|) = 0.$$

which yields that

$$S_{11} = S_{12}, U_{21} = U_{22}, C_{31} = C_{32}, C_{a(41)} = C_{a(42)}, R_{51} = R_{52}, B_{61} = B_{62}.$$

This completes the proof of uniqueness. If we use the Adams-Moulton rule for Atangana-Baleanu fractional integral to indicate the mathematical strategies then

$${}_0^{AB}I_t^{\alpha}[f(t_{w+1})] = \frac{1-\alpha}{B(\alpha)} + \frac{\alpha}{\Gamma(\alpha)} \sum_{j=0}^{\infty} [\frac{f(t_{w+1}) - f(t_w)}{2}] d_j^{\alpha}, \tag{3.16}$$

where

$$d_j^{\alpha} = (j+1)^{1-\alpha} - (j)^{1-\alpha.}$$

We obtain the following for the system 3.1:

$$\begin{aligned} S_{(w+1)}(t) - S_w(0) = S_0^w(t) + \frac{1-\alpha}{B(\alpha)}\Big[H - \Big(\frac{\lambda(t_{w+1}) - \lambda(t_n)}{2}\Big)\Big(\frac{S(t_{w+1}) - S(t_w)}{2}\Big) \\ -b\Big(\frac{S(t_{w+1}) - S(t_w)}{2}\Big)\Big] + \frac{\alpha}{\Gamma(\alpha)} \sum_{j=0}^{\infty} d_j^{\alpha}\Big[H - \Big(\frac{\lambda(t_{w+1}) - \lambda(t_w)}{2}\Big)\Big(\frac{S(t_{w+1}) - S(t_w)}{2}\Big) \\ -b\Big(\frac{S(t_{w+1}) - S(t_w)}{2}\Big)\Big], \end{aligned}$$

$$\begin{aligned} U_{(w+1)}(t) - U_w(0) = U_0^w(t) + \frac{1-\alpha}{B(\alpha)}\Big[\Big(\frac{\lambda(t_{w+1}) - \lambda(t_w)}{2}\Big)\Big(\frac{S(t_{w+1}) - S(t_w)}{2}\Big) \\ -(\rho+b)\Big(\frac{U(t_{w+1}) - U(t_w)}{2}\Big)\Big] + \frac{\alpha}{\Gamma(\alpha)} \sum_{j=0}^{\infty} d_j^{\alpha}\Big[\Big(\frac{\lambda(t_{w+1}) - \lambda(t_w)}{2}\Big)\Big(\frac{S(t_{w+1}) - S(t_w)}{2}\Big) \\ -(\rho+b)\Big(\frac{U(t_{w+1}) - U(t_w)}{2}\Big)\Big], \end{aligned}$$

$$\begin{aligned} C_{(w+1)}(t) - C_w(0) = C_0^w(t) + \frac{1-\alpha}{B(\alpha)}\Big[\rho(1-\tau)\Big(\frac{U(t_{w+1}) - U(t_w)}{2}\Big) - (b + c_1 + d_1)\Big(\frac{C(t_{w+1}) - C(t_w)}{2}\Big)\Big] \\ +\frac{\alpha}{\Gamma(\alpha)} \sum_{j=0}^{\infty} d_j^{\alpha}\Big[\rho(1-\tau)\Big(\frac{U(t_{w+1}) - U(t_w)}{2}\Big) - (b + c_1 + d_1)\Big(\frac{C(t_{w+1}) - C(t_w)}{2}\Big)\Big], \end{aligned}$$

$$\begin{aligned} C_{a(w+1)}(t) - C_{a(w)}(0) = C_{a(0)}^w(t) + \frac{1-\alpha}{B(\alpha)}\Big[\tau\rho\Big(\frac{U(t_{w+1}) - U(t_w)}{2}\Big) - (b + d_2)\Big(\frac{C_a(t_{w+1}) - C_a(t_w)}{2}\Big)\Big] \\ +\frac{\alpha}{\Gamma(\alpha)} \sum_{j=0}^{\infty} d_j^{\alpha}\Big[\phi_1\Big(\frac{U(t_{w+1}) - U(t_w)}{2}\Big) + \phi_2\Big(\frac{C(t_{w+1}) - C(t_w)}{2}\Big) + \phi_3\Big(\frac{C_a(t_{w+1}) - C_a(t_w)}{2}\Big) \end{aligned}$$

$$-\sigma\Big(\frac{B(t_{w+1})-B(t_w)}{2}\Big)\Big],$$

$$R_{(w+1)}(t)-R_w(0)=R_0^w(t)+\frac{1-\alpha}{B(\alpha)}\Big[d_1\Big(\frac{C(t_{w+1})-C(t_w)}{2}\Big)+d_2\Big(\frac{C_a(t_{w+1})-C_a(t_w)}{2}\Big)$$
$$-b\Big(\frac{R(t_{w+1})-R(t_w)}{2}\Big)\Big]+\frac{\alpha}{\Gamma(\alpha)}\sum_{j=0}^{\infty}d_j^{\alpha}\Big[d_1\Big(\frac{C(t_{w+1})-C(t_w)}{2}\Big)+d_2\Big(\frac{C_a(t_{w+1})-C_a(t_w)}{2}\Big)$$
$$-b\Big(\frac{R(t_{w+1})-R(t_w)}{2}\Big)\Big],$$

$$B_{(w+1)}(t)-B_w(0)=B_0^w(t)+\frac{1-\alpha}{B(\alpha)}\Big[\phi_1\Big(\frac{U(t_{w+1})-U(t_w)}{2}\Big)+\phi_2\Big(\frac{C(t_{w+1})-C(t_w)}{2}\Big)$$
$$+\phi_3\Big(\frac{C_a(t_{w+1})-C_a(t_w)}{2}\Big)-\sigma\Big(\frac{B(t_{w+1})-B(t_w)}{2}\Big)\Big]+\frac{\alpha}{\Gamma(\alpha)}\sum_{j=0}^{\infty}d_j^{\alpha}\Big[\phi_1\Big(\frac{U(t_{w+1})-U(t_w)}{2}\Big)$$
$$+\phi_2\Big(\frac{C(t_{w+1})-C(t_w)}{2}\Big)+\phi_3\Big(\frac{C_a(t_{n+1})-C_a(t_w)}{2}\Big)-\sigma\Big(\frac{B(t_{n+1})-B(t_w)}{2}\Big)\Big].$$

An operator $\hbar : E \to E$ can be set out as:

$$\hbar(\Delta)(t)=\Delta(0)+\frac{\vartheta t^{\vartheta-1}(1-\varpi)}{AB(\varpi)}\mho(t,\Delta(t))+\frac{\varpi\vartheta}{AB(\varpi)\Gamma(\varpi)}\int_0^t\lambda^{\vartheta-1}(t-\lambda)^{\vartheta-1}\mho(t,\Delta(t))d\lambda \tag{3.17}$$

For $\mho(t,\Delta(t))$ that attains the development and Lipscitz condition, so for $\Delta \in Z$ $\exists$ positive constants $E_{\mho},\ F_{\mho}$ such that

$$\mho(t,\Delta(t))\le E_{\mho}|\Delta(t)|+F_{\mho}. \tag{3.18}$$

Also, for $\Delta,\ \hat{\Delta} \in Z$ $\exists$ constant $G_{\mho}>0$ such that

$$|\mho(t,\Delta(t))-\mho(t,\hat{\Delta(t)})|\le G_{\mho}|\Delta(t)-\hat{\Delta}(t))|. \tag{3.19}$$

Theorem 4. If the state defined in (3.18) is true and by assuming the continuous function $\mho : [0,\tau]\times X\to R$ then it has unique outcome.

Proof. In the beginning, we reveal that $\hbar$ is completely continuous that are explained in (3.17). while $\mho$ is a continuous function, so $\hbar$ is also continuous function. Consider $J=\{\Delta \in X : \|\Delta\|\le R,\ R>0\}$. For any $\Delta \in X$, we have

$$\hbar(\Delta)(t)=max_{t\in[0,\tau]}|\Delta(0)+\frac{\vartheta t^{\vartheta-1}(1-\varpi)}{AB(\varpi)}\mho(t,\Delta(t))+\frac{\varpi\vartheta}{AB(\varpi)\Gamma(\varpi)}\int_0^t\lambda^{\vartheta-1}(t-\lambda)^{\vartheta-1}\mho(t,\Delta(t))d\lambda|$$
$$\le\Delta(0)+\frac{\vartheta\tau^{\vartheta-1}(1-\varpi)}{AB(\varpi)}(E_{\mho}\|\Delta\|+M_{\mho})+max_{t\in[0,\tau]}\frac{\varpi\vartheta}{AB(\varpi)\Gamma(\varpi)}\int_0^t\lambda^{\vartheta-1}(t-\lambda)^{\vartheta-1}|\mho(t,\Pi(t))d\lambda|$$
$$\le\Delta(0)+\frac{\vartheta\tau^{\vartheta-1}(1-\varpi)}{AB(\varpi)}(E_{\mho}\|\Delta\|+F_{\mho})+\frac{\varpi\vartheta}{AB(\varpi)\Gamma(\varpi)}(E_{\mho}\|\Delta\|+F_{\mho})\tau^{\varpi+\vartheta-1}H(\upsilon+\vartheta)$$

$$\leq R.$$

Hence, $\hbar$ is uniformly bounded, and $J(\varpi+\vartheta)$ representing the beta function.

For equicontinuity of $\hbar$, we take $t_1 < t_2 \leq \tau$. Then consider

$$\hbar(\Delta)(t_2)-\hbar(\Delta)(t_1) = |\frac{\vartheta t_2^{\vartheta-1}(1-\varpi)}{AB(\varpi)}\mho(t_2,\Delta(t_2))+\frac{\varpi\vartheta}{AB(\varpi)\Gamma(\varpi)}\int_0^{t_2}\lambda^{\vartheta-1}(t_2-\lambda)^{\vartheta-1}\mho(t,\Delta(t))d\lambda$$

$$-\frac{\vartheta t_1^{\vartheta-1}(1-\varpi)}{AB(\varpi)}\mho(t_1,\Delta(t_1))+\frac{\varpi\vartheta}{AB(\varpi)\Gamma(\varpi)}\int_0^{t_1}\lambda^{\vartheta-1}(t_1-\lambda)^{\vartheta-1}\mho(t,\Delta(t))d\lambda|$$

$$\leq \frac{\vartheta t_2^{\vartheta-1}(1-\varpi)}{AB(\varpi)}(L_\mho|\Delta(t)|,M_\mho)+\frac{\varpi\vartheta}{AB(\varpi)\Gamma(\varpi)}(E_\mho|\Delta(t)|,F_\mho)t_2^{\varpi+\vartheta-1}H(\varpi+\vartheta)$$

$$-\frac{\vartheta t_1^{\vartheta-1}(1-\varpi)}{AB(\varpi)}(E_\mho|\Delta(t)|,F_\mho)-\frac{\varpi\vartheta}{AB(\varpi)\Gamma(\varpi)}(E_\mho|\Delta(t)|,F_\mho)t_1^{\varpi+\vartheta-1}H(\varpi+\vartheta),$$

If $t_1 \to t_2$ then $||\hbar(\Delta)(t_2) - \hbar(\Delta)(t_1) \to 0||$.
Consequently $||\hbar(\Delta)(t_2) - \hbar(\Delta)(t_1) \to 0||$, as $t_1 \to t_2$. Thus, $\hbar$ is completely continuous by theorem of Arzela-Ascoli

Thus, $\hbar$ is equicontinuous and under the condition of Arzela-Ascoli theorem it is completely continuous. Consequently, the following result of Schauder's fixed point, it has at least one solution.

Theorem 5. By assuming the condition (3.19) is accurate and $\rho = (\frac{\vartheta\tau^{\vartheta-1}(1-\varpi}{AB(\varpi)} + \frac{\varpi\vartheta}{AB(\varpi)\Gamma(\varpi)}\tau^{\varpi+\vartheta-1}J(\varpi+\vartheta))I_\mho$ then for $\rho < 1$ gives a sole outcome.

For Δ, $\hat{\Delta} \in X$, we have

$$|\hbar(\Delta),\hbar\hat{\Delta}| = max_{t\in[0,\tau]}|+\frac{\vartheta t^{\vartheta-1}(1-\varpi)}{AB(\varpi)}[(\mho(t,\Delta(t))-\mho(t,\hat{\Delta(t)})]$$

$$+\frac{\varpi\vartheta}{AB(\varpi)\Gamma(\varpi)}\int_0^t\lambda^{\vartheta-1}(t-\lambda)^{\vartheta-1}d\lambda\mho(\lambda,\hat{\Delta(\lambda)})|$$

$$\leq\left[\frac{\vartheta\tau^{\vartheta-1}(1-\varpi)}{AB(\varpi)}+\frac{\varpi\vartheta}{AB(\varpi)\Gamma(\varpi)}\tau^{\varpi+\vartheta-1}H(\varpi,\vartheta)\right]||\hbar(\Delta)-\hbar(\hat{\Delta})||$$

$$\leq\rho||\hbar(\Delta)-\hbar(\hat{\Delta})||.$$

Thus, $\hbar$ has contraction and by using the Banach contraction principle, it has a special outcome.

4. Simulation and Discussion

In the simulation of a model, parameters have a key contribution. Here we use the actual data of Saudi Arabia having parameters values given in [38]. After that, we have spreading rates of the uncovered (μ_1), symptomatic (μ_2), asymptomatic (μ_3), and environment (μ_4) are 0.2259, 0.1298, 0.4579, 0.0969, respectively. Further, we got the values of the incubation period ($\rho = 0.1141$), asymptotically infected persons ($\tau = 0.3346$), the Improvement rate of C ($d_1 0.3346$), and the improvement rate of C_a ($d_2 = 0.0867$). The parameters $\phi_1 = 0.2616$, $\phi_1 = 0.0100$, $\phi_1 = 0.1815$, $\sigma = 0.2786$ represents the contribution caused by U, C, Ca, destruction of virus. We presented the simulation data in Figures 1–6 with several values of fractional order (α). In Figures 1–3, 5 and 6, we will observe that $S(t)$, $U(t)$, $C(t)$, $C_a(t)$ and $B(t)$ population increase with decreasing the fractional order α where as $R(t)$ start decreasing by decreasing fractional values. It is observed that the decrease in pandemic peaks is comparatively faster for smaller values of α as shown in Figures 1–6. Fractional parameter shows the study of COVID-19 outbreak continuously from starting place to their end boundary. It can be easily seen that the COVID-19 spread is more and more and recovery rate reduces from the actual data of Saudi Arabia when study it by every smaller region. This type study will help us locate the rate of actual number of infected people. The impact of memory index α on the dynamics of virus concentration in the environment at α is analyzed to check the outbreak of this pandemic.

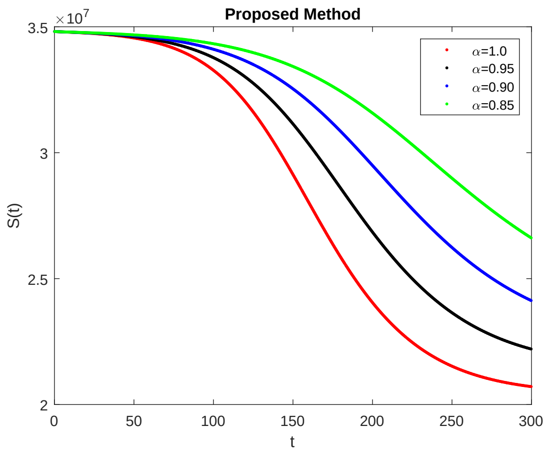

Figure 1. Simulation of S(t) proposed fractional order operator.

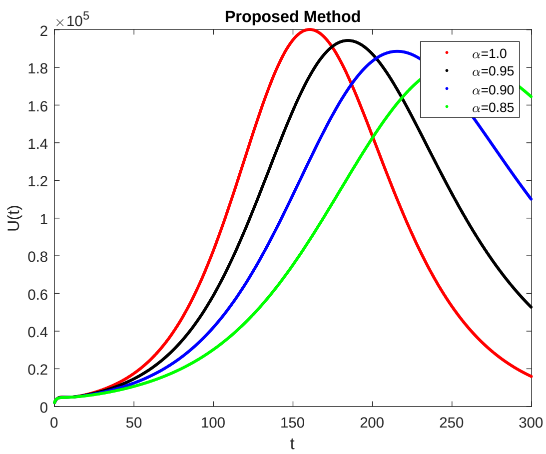

Figure 2. Simulation of U(t) proposed fractional order operator.

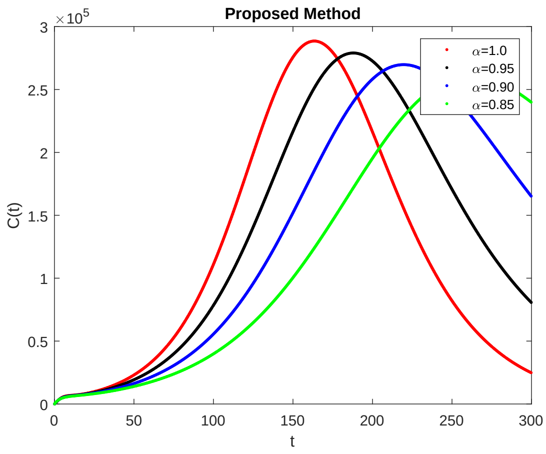

Figure 3. Simulation of C(t) proposed fractional order operator.

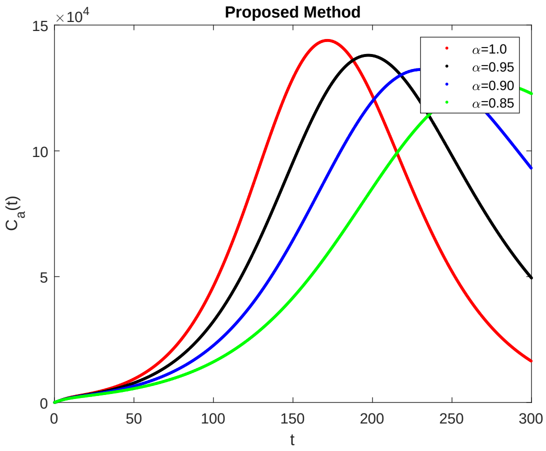

Figure 4. Simulation of $C_a(t)$ proposed fractional order operator.

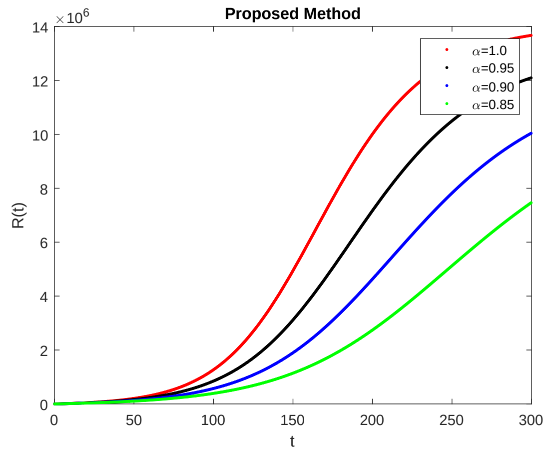

Figure 5. Simulation of R(t) proposed fractional order operator.

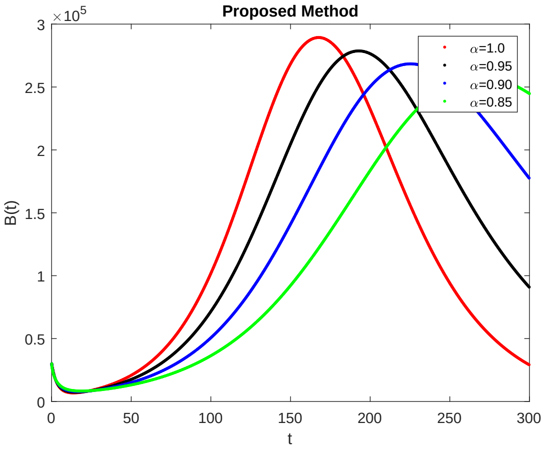

Figure 6. Simulation of B(t) proposed fractional order operator.

5. Conclusions

Mathematical modeling plays an important role to control, planning and reduce the bad impact of infectious disease in the society from last decays. Results of fractional order model have a memory effect on epidemic model as compared to classical model. In this formation, results show that contaminated parts are reduced by lowering the fractional order. Some notional outcomes are produced for the model to demonstrate the productivity of the created procedures.Graphical representation indicates that we can reduce the cases rapidly if communities of the country follow some rules, including social distance, cleaning their hands, keeping away from the throng. Theoretical results are investigated for the fractional-order model, which proved the efficiency of the developed schemes. Numerical simulation has been made to check the actual behavior of the COVID-19 outbreak. Such type of study will be helpful in future to understand the outbreak of this epidemic and to control the disease in a community. The power of these component operators is their non-local features that are not in the integer separator operator. Separated features of differentiated statistics define the memory and transfer structures of many mathematical models. As a reality that fractional order models are more practical and beneficial than classical integer order models. Fractional order findings produce a greater degree of freedom in these models. Unnecessary order outscoring is powerful tools for understanding the dynamic behavior of various bio objects and systems.

Acknowledgments

National Natural Science Foundation of China (No. 71601072), Key Scientific Research Project of Higher Education Institutions in Henan Province of China (No. 20B110006) and the Fundamental Research Funds for the Universities of Henan Province, China (No. NS-FRF210314).

Conflict of interest

The authors declare that they have no competing interests.

References

1. I. Podlubny, *Fractional differential equations: An introduction to fractional derivatives, fractional differential equations, to methods of their solution and some of their applications*, Elsevier, 1998.
2. A. Atangana, Non validity of index law in fractional calculus, a fractional differential operator with markovian and non-markovian properties, *Physica A*, **505** (2018), 688–706. http://dx.doi.org/10.1016/j.physa.2018.03.056
3. D. Baleanu, A. Jajarmi, E. Bonyah, M. Hajipour, New aspects of poor nutrition in the life cycle within the fractional calculus, *Adv. Differ. Equ.*, **2018** (2018), 230. http://dx.doi.org/10.1186/s13662-018-1684-x
4. S. Ullah, M. A. Khan, M. Farooq, A fractional model for the dynamics of TB virus, *Chaos Soliton. Fract.*, **116** (2018), 63–71. http://dx.doi.org/10.1016/j.chaos.2018.09.001
5. S. Ullah, M. A. Khan, M. Farooq, Modeling and analysis of the fractional HBV model with atangana-baleanu derivative, *Eur. Phys. J. Plus*, **133** (2018), 313. http://dx.doi.org/10.1140/epjp/i2018-12120-1
6. Fatmawati, M. A. Khan, M. Azizah, Windarto, S. Ullah, A fractional model for the dynamics of competition between commercial and rural banks in indonesia, *Chaos Soliton. Fract.*, **122** (2019), 32–46. http://dx.doi.org/10.1016/j.chaos.2019.02.009
7. M. Farman, M. U. Saleem, M. F. Tabassum, A. Ahmad, M. O. Ahmad, A linear control of composite model for glucose insulin glucagon, *Ain Shams Eng. J.*, **10** (2019), 867–872. http://dx.doi.org/10.1016/j.asej.2019.04.001
8. K. A. Golmankhaneh, C. Tunç, Sumudu transform in fractal calculus, *Appl. Math. Comput.*, **350** (2019), 386–401. http://dx.doi.org/10.1016/j.amc.2019.01.025
9. M. Goyal, H. Mehmet Baskonus, A. Prakash, An efficient technique for a time fractional model of lassa hemorrhagic fever spreading in pregnant women, *Eur. Phys. J. Plus*, **134** (2019), 482. http://dx.doi.org/10.1140/epjp/i2019-12854-0
10. S. Zhao, H. Chen, Modeling the epidemic dynamics and control of covid-19 outbreak in China, *Quant. Biol.*, **8** (2020), 11–19. http://dx.doi.org/10.1007/s40484-020-0199-0
11. S. Ullah, M. A. Khan, M. Farooq, Z. Hammouch, D. Baleanu, A fractional model for the dynamics of tuberculosis infection using caputo-fabrizio derivative, *Discrete Cont. Dyn. Sys. S*, **13** (2020), 975–993. http://dx.doi.org/10.3934/dcdss.2020057
12. M. A. Khan, A. Atangana, Modeling the dynamics of novel coronavirus (2019-ncov) with fractional derivative, *Alex. Eng. J.*, **59** (2020), 2379–2389. http://dx.doi.org/10.1016/j.aej.2020.02.033
13. M. Rahman, M. Arfan, k. Shah, J. F. Gómez-Aguilar, Investigating a nonlinear dynamical model of covid-19 disease under fuzzy Caputo, random and ABC fractional-order derivative, *Chaos Soliton. Fract.*, **140** (2020), 110232. http://dx.doi.org/10.1016/j.chaos.2020.110232
14. N. H. Tuan, H. Mohammadi, S. Rezapour, A mathematical model for covid-19 transmission by using the Caputo fractional derivative, *Chaos Soliton. Fract.*, **140** (2020), 110107. http://dx.doi.org/10.1016/j.chaos.2020.110107

15. F. S. Alshammari, A mathematical model to investigate the transmission of COVID-19 in the kingdom of Saudi Arabia, *Comput. Math. Methods Med.*, **2020** (2020), 9136157. http://dx.doi.org/10.1155/2020/9136157

16. A. Prakash, M. Goyal, H. M. Baskonus, S. Gupta, A reliable hybrid numerical method for a time dependent vibration model of arbitrary order, *AIMS Mathematics*, **5** (2020), 979–1000. http://dx.doi.org/10.3934/math.2020068

17. C. Tunc, A. K. Golmankhaneh, On stability of a class of second alpha-order fractal differential equations, *AIMS Mathematics*, **5** (2020), 2126–2142. http://dx.doi.org/10.3934/math.2020141

18. M. Hamid, M. Usman, R. U. Haq, W. Wang, A Chelyshkov polynomial based algorithm to analyze the transport dynamics and anomalous diffusion in fractional model, *Physica A*, **551** (2020), 124227. http://dx.doi.org/10.1016/j.physa.2020.124227

19. M. Goyal, H. M. Baskonus, A. Prakash, Regarding new positive, bounded and convergent numerical solution of nonlinear time fractional HIV/AIDS transmission model, *Chaos Soliton. Fract.*, **139** (2020), 110096. http://dx.doi.org/10.1016/j.chaos.2020.110096

20. M. Hamid, M. Usman, W. Wang, Z. Tian, Hybrid fully spectral linearized scheme for time-fractional evolutionary equations, *Math. Meth. Appl. Sci.*, **44** (2021), 3890–3912. http://dx.doi.org/10.1002/mma.6996

21. M. Farman, M. U. Saleem, A. Ahmad, S. Imtiaz, M. F. Tabassum, S. Akram, et al., A control of glucose level in insulin therapies for the development of artificial pancreas by Atangana Baleanu fractional derivative, *Alex. Eng. J.*, **59** (2020), 2639–2648. http://dx.doi.org/10.1016/j.aej.2020.04.027

22. M. U. Saleem, M. Farman, A. Ahmad, E. U. Haque, M. O. Ahmad, A Caputo Fabrizio fractional order model for control of glucose in insulintherapies for diabetes, *Ain Shams Eng. J.*, **11** (2020), 1309–1316. http://dx.doi.org/10.1016/j.asej.2020.03.006

23. M. Farman, A. Akgül, A. Ahmad, D. Baleanu, M. U. Saleem, Dynamical transmission of coronavirus model with analysis and simulation, *CMES-Comput. Model. Eng. Sci.*, **127** (2021), 753–769. http://dx.doi.org/10.32604/cmes.2021.014882

24. M. Farman, A. Ahmad, A. Akgül, M. U. Saleem, M. Naeem, D. Baleanu, Epidemiological analysis of the coronavirus disease outbreak with random effects, *CMC-Comput. Mater. Con.*, **67** (2021), 3215–3227. http://dx.doi.org/10.32604/cmc.2021.014006

25. M. Aslam, M. Farman, A. Akgül, M. Sun, Modeling and simulation of fractional order COVID-19 model with quarantined-isolated people, *Math. Meth. Appl. Sci.*, **44** (2021), 6389–6405. http://dx.doi.org/10.1002/mma.7191

26. M. Aslam, M. Farman, A. Akgül, A. Ahmad, M. Sun, Generalized form of fractional order COVID-19 model with Mittag-Leffler kernel, *Math. Meth. Appl. Sci.*, **44** (2021), 8598–8614. http://dx.doi.org/10.1002/mma.7286

27. M. Bohner, O. Tunç, C. Tunç, Qualitative analysis of caputo fractional integro-differential equations with constant delays, *Comp. Appl. Math.*, **40** (2021), 214. http://dx.doi.org/10.1007/s40314-021-01595-3

28. V. Padmavathi. A. Prakash, K. Alagesan, N. Magesh, Analysis and numerical simula-tion of novel coronavirus (COVID-19) model with Mittag-Leffler Kernel, *Math. Meth. Appl. Sci.*, **44** (2021), 1863–1877. http://dx.doi.org/10.1002/mma.6886

29. M. Usman, M. Hamid, M. Liu, Novel operational matrices-based finite difference/spectral algorithm for a class of time-fractional Burger equation in multidimensions, *Chaos Soliton. Fract.*, **144** (2021), 110701. http://dx.doi.org/10.1016/j.chaos.2021.110701

30. A. Prakash, H. Kaur, Analysis and numerical simulation of fractional Biswas–Milovic model, *Math. Comput. Simulat.*, **181** (2021), 298–315. http://dx.doi.org/10.1016/j.matcom.2020.09.016

31. M. Hamid, M. Usman, R. Haq, Z. Tian, A spectral approach to analyze the nonlinear oscillatory fractional-order differential equations, *Chaos Soliton. Fract.*, **146** (2021), 110921. http://dx.doi.org/10.1016/j.chaos.2021.110921

32. M. Mehmood, M. Hamid, S. Ashraf, Z. Tian, Galerkin time discretization for transmission dynamics of HBV with non-linear saturated incidence rate, *Appl. Math. Comput.*, **410** (2021), 126481. http://dx.doi.org/10.1016/j.amc.2021.126481

33. M. Amin, M. Farman, A. Akgül, R. T. Alqahtani, Effect of vaccination to control COVID-19 with fractal fractional operator, *Alex. Eng. J.*, **61** (2022), 3551–3557. http://dx.doi.org/10.1016/j.aej.2021.09.006

34. M. Higazy, F. M. Allehiany , E. E. Mahmoud, Numerical study of fractional order COVID-19 pandemic transmission model in context of ABO blood group, *Results Phys.*, **22** (2021), 103852. http://dx.doi.org/10.1016/j.rinp.2021.103852

35. M. Caputo, M. Fabrizio, A new definition of fractional derivatives without singular kernel, *Prog. Fract. Differ. Appl.*, **1** (2015), 1–13.

36. A. Atangana, D. Baleanu, New fractional derivatives with nonlocal and non-singular kernel theory and application to heat transfer model, *Therm. Sci.*, **20** (2016), 763–769.

37. A. Atangana, E. Bonyah, A. A. Elsadany, A fractional order optimal 4D chaotic financial model with Mittag-Leffler law, *Chinese J. Phys.*, **65** (2020), 38–53. http://dx.doi.org/10.1016/j.cjph.2020.02.003

38. E. Alzahrani, M. M. El-Dessoky, D. Baleanu, Mathematical modeling and analysis of the novel Coronavirus using Atangana-Baleanu derivative, *Results Phys.*, **25** (2021), 104240. http://dx.doi.org/10.1016/j.rinp.2021.104240